Photonic band-gap properties of a porous silicon periodic planar waveguide

Patrick Ferrand, R. Romestain, J.-C. Vial

Photonic band-gap properties of a porous silicon periodic planar waveguide

P. Ferrand, R. Romestain, and J. C. Vial
Laboratoire de Spectrométrie Physique, Université J. Fourier Grenoble 1, CNRS UMR 5588, Boîte Postale 87, F-38402 Saint Martin d'Hères Cedex, France
(Received 4 September 2000; published 26 February 2001)

We have elaborated a photonic band-gap structure based on nanoporous silicon, structured both in depth and in plane with a 0.45-μm period. Near infrared continuous transmittance spectra, compared to calculations performed by means of a coupled-mode theory, allow quantitative measurements of the optical index both in the plane and in depth, and demonstrate that the final material index is modulated up to $\Delta n = 0.5$. Wide ($\Delta\lambda/\lambda \approx 0.1$ in TM, 0.05 in TE) and efficient stop bands are measured. They are attributed to a strong selectivity at the edge coupling.

DOI: 10.1103/PhysRevB.63.115106 PACS number(s): 42.70.Qs, 42.40.Eq, 42.79.Gn, 78.66.Jg

Since it has been demonstrated that they can modify the propagation of electromagnetic waves as a crystal modifies the motion of electrons,[1,2] periodic index media are the subject of intense work. However, due to the technological challenge to perform a submicronic structuration, experimental evidence has been only obtained recently at optical wavelengths on a planar structure.[3]

In this context, porous silicon (PS) plays a promising role: Macro-PS allows us to obtain a regular pattern of air cylinders in bulk silicon, on a depth of several hundreds of microns, and a complete two-dimensional photonic band gap has been demonstrated in the mid-infrared[4] and recently in the near infrared (NIR)[5]. On the other hand, nano-PS is very well adapted to index modulations in depth. Multilayers can constitute efficient distributed Bragg reflectors,[6] and a confinement of light along one dimension has been demonstrated by realizing planar microcavities.[7] Moreover, a holographic process has been used in order to obtain nano-PS that is periodically structured in the plane.[8]

In this paper, we demonstrate a nano-PS photonic structure, with an optical index structured for the first time to our knowledge both in depth, in order to confine the light, and along one direction of plane with a submicronic periodical index along one direction of plane. Photonic properties are investigated by transmission measurements of edge-coupled guided light in a wide continuous range in the NIR, and by means of the coupled-wave theory. The use of a multimode waveguide allows quantitative measurements of the optical indices, both in the plane and in depth.

Our samples were obtained by a two-step process. First, planar waveguides were made by etching two successive nano-PS layers with different porosities. We used low doped p type (100) Si substrates (4 Ω cm), with a thickness of only 100 μm, to allow perfect cleaved edges. The 1.6-μm-thick upper (guiding) layer and the 4.5-μm-thick lower (cladding) layer were made using a $HF:H_2O:C_2H_5OH$ (35:35:30) solution at room temperature, and current densities of 16.6 mA cm^{-2} and 50 mA cm^{-2}, in order to obtain respective porosities of 58% and 65%.

Then, after the etching, a holographic grating of period Λ was obtained by leaving the sample in its electrolyte and by illuminating during 8 min its total surface area by the interference pattern produced by two coherent spatially-filtered TE-polarized expanded beams of a Ar^+ ion laser ($\lambda = 0.5145$ μm). Typical power density for each beam was 20 mW cm^{-2}. We took care to form the grating parallel to the final cleaved edges. The period is precisely determined by measuring accurately the diffraction angle of a laser beam.

Transmitted spectrum of guided light were performed by end-fire coupling. White light from a straight tungsten filament chopped with a mechanical device was coupled into and out of the sample using two Cassegrain reflecting microscope objectives (25×, numerical aperture = 0.4 and 15×, numerical aperture = 0.28) in order to be perfectly achromatic. Due to the central obscuration of this kind of objectives, we chose to rotate the sample in its plane and then to use only the half part of beam that is normal to the sample edge. The angular aperture in the plane of the sample is then typically $\pm 5°$. Using a beamsplitter, the output edge was imaged onto both a NIR camera and the entrance slit of a 1200 gr/mm monochromator (gr denotes groove). The polarization was selected by a polarizer inserted in front of the monochromator. The signal was acquired by a cooled InGaAs photomultiplier, and measured through a lock-in amplifier. All experimental spectra were corrected by the spectral response of the detection system, which was measured by imaging the filament without any sample.

We will follow the detailed coupled-wave theory presented in Ref. 9, generalized to the multimode case.[10] This perturbative method allows to treat the propagation and the interactions of guided modes in a periodic planar dielectric waveguide as shown in Fig. 1(a). It is based on the expansion of the total electric field in the discrete eigenmodes of the unperturbed waveguide, each one characterized by its propagation constant β_l, which gives the phase dependence in the z direction, with l a positive integer that indexes each mode. A Λ-periodic perturbation, expanded as

$$\Delta n^2(x,z) = \Delta n^2(x) \sum_{p=-\infty}^{+\infty} a_p \exp(ipQz), \qquad (1)$$

where Δn^2 is the perturbation of the square of the optical index n, and where $Q \equiv 2\pi/\Lambda$, can couple two guided modes β_l and β_m, if the diffraction condition,

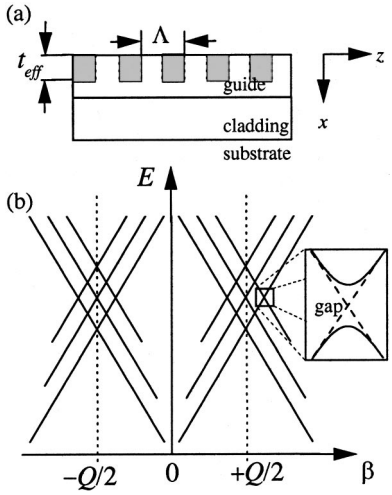

FIG. 1. Sketch (a) of a planar periodic multimode waveguide. The holographic process gives a periodic index along one direction of plane. This perturbation (gray pattern) has an effective depth t_{eff}. Typical dispersion curves (b) of this waveguide, reproduced with $\pm Q$ shifts, in order to take into account the periodicity. Coupling between modes is possible each time the curves cross: the degeneracy can be lifted, and a gap can appear, as illustrated in the inset.

$$\beta_l + pQ \approx \beta_m, \tag{2}$$

is verified for an integer p. The coupling efficiency depends on the coupling constant

$$\kappa_{lm}^{\mathrm{TE}} = \frac{i\omega\epsilon_0 a_p}{4}\int_0^{+\infty} \Delta n^2(x)\mathcal{E}_y^{(l)}(x)\mathcal{E}_y^{(m)}(x)\mathrm{d}x, \tag{3a}$$

or

$$\kappa_{lm}^{\mathrm{TM}} = \frac{-i\omega\mu_0 a_p}{4}\int_0^{+\infty} \frac{\Delta n^2(x)}{n^2(x)}\mathcal{H}_y^{(l)}(x)\mathcal{H}_y^{(m)}(x)\mathrm{d}x, \tag{3b}$$

where $\mathcal{E}_y^{(l)}$ and $\mathcal{H}_y^{(l)}$ are, respectively, the normalized values of electrical and magnetic field of the lth TE and TM eigenmodes of the unperturbed waveguide.

Dispersion curves of a periodic multimode waveguide are shown in Fig. 1(b). Each crossing means that modes propagating in opposite directions (signs of β_l and β_m are opposite) can be coupled into each other. Thus, in case of an efficient coupling, the degeneracy will be lifted and a gap will appear so that the modes β_l and β_m cannot exist in the structure for energies inside the gap. Considering only the coupling between two modes β_l and β_m, the power carried by an incident mode β_l will be attenuated after a perturbation on a length L by a transmission coefficient T_{lm}, given by

$$T_{lm} = \frac{2|SL|^2}{(\Delta\beta L)^2 f_-(SL) + |SL|^2 f_+(SL)}, \tag{4}$$

where $S=[|\kappa_{lm}|^2-(\Delta\beta)^2]^{1/2}$, $\Delta\beta=\frac{1}{2}(\beta_l-\beta_m+lQ)$, and $f_\pm(X+iY)=\cosh(2X)\pm\cos(2Y)$. Using Eq. (4), one can show that the stop-band width increases with the coupling constant.

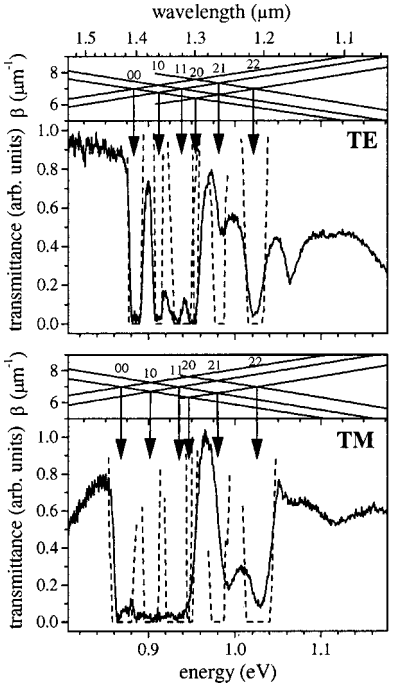

FIG. 2. Transmission spectra measured on a periodic nano-PS waveguide, reported for both TE and TM polarizations. The calculated crossing dispersion curves are also plotted at the top of each spectrum. Above each arrow, that shows the correspondence between crossings and stopbands, we reported the couple of integers lm that designate each coupling. Numerical calculation (dashed) of the transmission coefficient T of each mode-coupling are superposed to experimental data.

Experimental transmission spectra of a periodic nano-PS multimode waveguide of length $L=1.3$ mm, and period $\Lambda=0.45$ μm have been performed in a wide continuous spectral range in the NIR, for TE and TM polarizations, and reported in Fig. 2. They show several stop bands, for which the intensity decreases down to two orders of magnitude. Measurements were compared to calculations, performed by means of the coupled-mode theory described above. During the holographic process, the photodissolution is localized and is related to the power density of light.[11] In order to take into account both the interference pattern in the plane and the attenuation of light in depth, due to the absorption in nano-PS, we modelized the optical index perturbation, for $x>0$, as

$$\Delta n^2(x,z) = \Delta n_0^2 \exp(-x/t_{\mathrm{eff}})\cos^2(Qz/2), \tag{5}$$

where t_{eff} represents the effective depth of illumination. All possible mode crossings were calculated using Eq. (3a) or (3b), and the transmitted intensity using Eq. (4). The index dispersion, very weak in the NIR range, was neglected. Following the experimental evidence for optical anisotropy,[12] we considered nano-PS as a positive uniaxial material with the optical axis normal to the layer surface, with ordinary and extraordinary indices n_o and n_e,[14] viewed, respectively, by the components of field in the plane and normal to the surface.

Using only one set of these parameters, we tried to obtain the best fit between experiment and calculations. This in-

TABLE I. Numerical values used to calculate dispersion curves and transmission spectra plotted in Fig. 2.

	n_o	n_e
Guide	1.59	1.63
Cladding	1.31	1.32
	TE	TM
Δn_0	−0.2	−0.5
t_{eff} (μm)	0.5	0.5

cludes the dispersion curves—for which each crossing has to be related to a stop band—and all stop band spectral positions and widths. The different stop bands have been calculated only by changing the modes that are coupled into each others, i.e., by choosing integers l and m in Eq. (2). The values of parameters are reported in Table I.

The best fit that is able to reproduce in the same time the spectral (absolute and relative) position and the width of each stop band is reported in Fig. 2. However, some effects remain unexplained: the sharp decrease of intensity, near 1.07 eV in TE polarization cannot be attributed to any mode coupling and the 0.98 eV calculated stop band is less pronounced on experimental data, especially in TE polarization. Nevertheless, the low number of parameters gives a very satisfying fit.

The stop-band width is related to both Δn_0^2 and t_{eff} via the coupling constant. However, these parameters can be estimated separately, because they do not play the same role. Especially, the coupling between modes for which $l \neq m$ depends strongly on the effective thickness t_{eff}. Indeed, if Δn^2 is nearly constant in depth, i.e., t_{eff} is large compared to the thickness of the guiding layer, integrals of Eqs. (3) become very small if $l \neq m$, due to orthogonality between unperturbed eigenmodes.[9] This is not the case if the periodic modulation is limited only at the top of the guiding layer. However, the reasons for which the absorption value of 2 μm^{-1}—suggested by the value of t_{eff}—is slightly larger than the value ($\approx 0.5\ \mu\text{m}^{-1}$) obtained by the rigorous analysis of reflectance spectra of dried samples, are not clear at the moment.

Another point is that the stop bands in TM polarization are so wide that they overlap. Spectra have been measured at normal incidence, thus angular effects[15] cannot be invoked. Thus, the broadness was attributed to a larger index perturbation, viewed from the vertical component of field. Such anisotropy effects due to the illumination of samples by polarized light during their etching have already been reported.[13]

The external azimuth angle ϕ has also been varied by rotating the sample in its plane. Spectra are reported in Fig. 3, for several values of ϕ up to 30°. Since the propagation constants β_l along the z direction become $\beta_l \cos(\phi_g)$, where ϕ_g is the azimuth angle inside the guiding layer determined by the guide index n_g, the wavelength of each stop band becomes $\lambda_{lm} \cos(\phi_g)$, where λ_{lm} is the wavelength of stop band at normal incidence. The angular dependence of λ_{lm} has been plotted for a selected stop band, and we reported on the same graph the calculations performed for index values

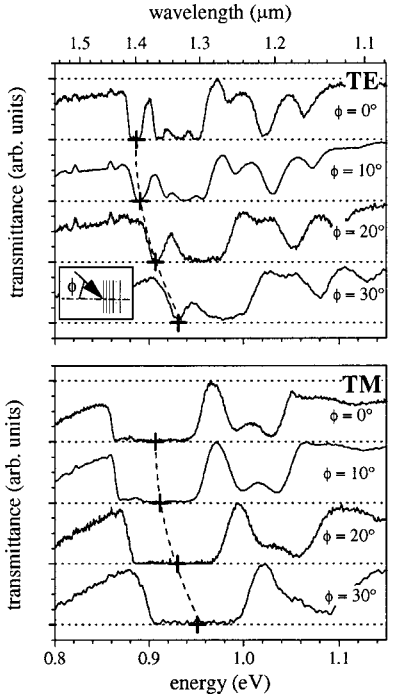

FIG. 3. Transmittance spectra measured for several azimuth angle ϕ. The crosses show the angular dependence of a selected stop band, dotted lines correspond to theoretical values obtained with a mean-index model. The azimuth angle ϕ is defined in the inset.

of the unperturbed waveguide given in Table I, i.e., we assumed $n_g \approx n_o$ in TE and $n_g \approx n_e$ in TM. The good agreement confirms that the index perturbation is weak: the entire guiding layer keeps a mean index value very close to its unperturbed value in spite of the strong perturbation near its top surface. This validates the use of a perturbative theory.

Furthermore, these measurements show an unexpected property of periodic multimode waveguides. A periodic structure on a multimode waveguide should perturb only the modes that verify the diffraction condition of Eq. (2). However, our measurements show unambiguously that in case of an efficient mode-coupling, e.g., for $(l,m)=(0,0)$, no power has been injected into modes otherwise allowed to propagate freely (e.g., $l=1$). Indeed, the coupled-mode theory has been developed to treat waveguides for which the perturbation is localized only in a region, so that the unperturbed eigenmodes really exist before and after the perturbation. But in our case, the perturbation covers the total sample surface, and another coupling occurs at the edge. This edge-coupling has to work directly with the external plane wave on one side and the modes of the periodic waveguide on the other side. In this case, the system (edge + periodic multimode waveguide) is found to possess a very wide stop band ($\Delta\lambda/\lambda \approx 0.1$ in TM, 0.05 in TE), even if the perturbation is weak. This is to our best knowledge the first experimental evidence for such a selective edge-coupling.

In conclusion, these results demonstrate that a photonic structure, consisting of an optical index modulated both in the plane and in depth, efficient in the near infrared, is fea-

sible using nanoporous silicon. A small period obtained ($0.45\ \mu$m), and a index contrast as large as 0.5 at the surface, have been obtained.[17] A three-beam holographic pattern, in order to obtain a hexagonal index lattice in the plane, would give an efficient control of light propagating along all directions of plane. Furthermore, the simultaneous use of a little absorbed wavelength, in order to have a deep perturbation, and a periodic modulation in depth will open a wide area of investigations in the realization of submicronic really three-dimensional structures. In addition, we have to stress the fact that the open porosity is a real plus, that could convert a passive structure into a high-performance host for various types of emitters.[16]

We wish to thank Dr. S. Setzu for her continued interest and useful discussions.

[1] E. Yablonovitch, Phys. Rev. Lett. **58**, 2059 (1987); S. John, *ibid.* **58**, 2486 (1987).

[2] J. D. Joannopoulos, R. D. Meade, and J. N. Winn, *Photonics Crystals: Molding the Flow of Light* (Princeton University Press, Princeton, NJ, 1995).

[3] D. Labilloy, H. Benisty, C. Weisbuch, T. Krauss, R. M. De La Rue, V. Bardinal, R. Houdré, U. Oesterle, D. Cassagne, and C. Jouanin, Phys. Rev. Lett. **79**, 4147 (1997).

[4] U. Grüning, V. Lehmann, S. Ottow, and K. Busch, Appl. Phys. Lett. **68**, 747 (1996).

[5] S. Rowson, A. Chelnokov, and J. M. Lourtioz, Electron. Lett. **35**, 753 (1999).

[6] G. Vincent, Appl. Phys. Lett. **64**, 2367 (1994).

[7] V. Pellegrini, A. Tredicucci, C. Mazzoleni, and L. Pavesi, Phys. Rev. B **52**, R14 328 (1995); S. Setzu, S. Létant, P. Solsona, R. Romestain, and J. C. Vial, J. Lumin. **80**, 129 (1999).

[8] G. Lérondel, R. Romestain, J. C. Vial, and M. Thönissen, Appl. Phys. Lett. **71**, 196 (1997).

[9] A. Yariv, *Quantum Electronics* (Wiley, New York, 1988); H. Stoll and A. Yariv, Opt. Commun. **8**, 5 (1973).

[10] E. Peral and A. Yariv, J. Lightwave Technol. **17**, 942 (1999).

[11] S. Létant and J. C. Vial, J. Appl. Phys. **80**, 7018 (1996).

[12] I. Mihalcescu, G. Lérondel, and R. Romestain, Thin Solid Films **297**, 245 (1997).

[13] G. Polisski, A. V. Adrianov, D. Kovalev, and F. Koch, Braz. J. Phys. **26**, 189 (1996).

[14] In case of anisotropy, in TM polarization, n^2 in Eq. (3b) has to be replaced by $n(\beta_l)n(\beta_m)$, where n depends on the propagating constant as $n(\beta)=n_o[1+(\beta/k)^2(n_o^{-2}-n_e^{-2})]^{1/2}$.

[15] It is well known that distributed Bragg reflectors used off-axis possess the broadest stop band when the electrical field stays perpendicular to the direction along which the index is periodic. In our case, where the periodicity is along the z direction [see Fig. 1(a)], this corresponds to the polarization called TM.

[16] S. Setzu, P. Solsona, S. Létant, R. Romestain, and J. C. Vial, Eur. Phys. J.: Appl. Phys. **7**, 59 (1999); H. Henley, Y. Koshka, J. Lagowski, and J. Siejka, J. Appl. Phys. **87**, 7848 (2000).

[17] These values show that the resolution of the holographic process is not strongly limited by the diffusion of the photocarriers.